Charmonium moving through a strongly coupled QCD plasma: a holographic perspective

Paul M. Hohler

Cyclotron Institute and Department of Physics & Astronomy,

Texas A& M University, College Station, TX 77843-3366, USA *

Yi Yin

Department of Physics, University of Illinois, Chicago, IL 60607-7059, USA †

arXiv:1305.1923v2 [nucl-th] 28 Oct 2013

Abstract

The properties of charmonium in a strongly coupled QCD-like plasma at finite momentum are studied. This is based upon a " bottom-up " holographic model which has been previously shown to reproduce charmonium phenomenology in vacuum and give a reasonable dissociation temperature at zero momentum. The finite momentum spectral functions are presented and found to be consistent with recent lattice results. The in-medium dispersion relation and momentum dependence of the decay width of J/ψ have also been investigated. We find no signature of a subluminal limiting velocity from the dispersion relation, while we note that the dissociation temperature decreases with momentum faster than previous holographic models. Based upon the dissociation temperature, a maximum momentum for J/ψ in-medium is identified and its phenomenological implications on J/ψ suppression are discussed

* pmhohler@comp.tamu.edu.edu

† yyin3@uic.edu

I. INTRODUCTION

The work of Matsui and Satz [1] introduced the idea of using heavy quarkonium as a probe of the formation of a strongly coupled quark gluon plasma (QGP). In the deconfined phase, $c\bar{c}$ bound states will dissociate because of color screening and thereby exhibit a suppression relative to the confined phase. This suppression can depend on momentum of the heavy quark pair and has been observed experimentally in heavy ion collisions [2–5]. To understand the experimentally observed suppression, it is important to understand equilibrium properties of charmonium (see, e.g., Ref. [6] for a recent review). In this paper, we will focus on one aspect of J/ψ suppression, namely the dissociation temperature.

In field theory, the basic quantity encoding the equilibrium properties of charmonium is the retarded Green's function $G^{\rm R}_{\mu\nu}(\omega,\boldsymbol{k}) \sim \langle J_\mu J_\nu\rangle$ or its spectral function $\rho(\omega,\boldsymbol{k})$. Here $J^\mu = \bar{c}\gamma^\mu c$ is the conserved heavy quark vector current operator. The dissociation of J/ψ can be attributed to the disappearance of the J/ψ peak in $\rho(\omega,\boldsymbol{k})$. In terms of the Green's function, the J/ψ peak is associated with a pole , $\Omega_{J/\psi}$, of $G^{\rm R}_{\mu\nu}(\omega,\boldsymbol{k})$ in the lower half of the complex ω plane[1]. The real part of this pole is the in-medium mass of J/ψ and determines the equilibrium abundance of J/ψ mesons, while the (minus) imaginary part of that pole is associated with the peak width, characterizing the interactions between J/ψ and the medium. Examining the pole structure of $G^{\rm R}_{\mu\nu}(\omega,\boldsymbol{k})$ is the equivalent to examining the peak structure of $\rho(\omega,\boldsymbol{k})$.

Due to strong coupling, the calculation of $G^{\rm R}_{\mu\nu}(\omega,\boldsymbol{k})$ in QCD at temperatures relevant to experiments is a challenging task. Recently, there have been effective field theory computations of quarkonia in the quark gluon plasma (see for example [7–9]), though these computations tend to be more applicable to the case of bottomonium rather than that of charmonium. Properties of heavy quarkonium in the medium have also been studied from first principle lattice QCD simulations, both at rest [10–12] and at finite momentum [13–16]. Similar calculations have also been preformed for bottomonium on the lattice [17]. However, being restricted to the finite interval of Euclidean time, determining real time correlator $G^{\rm R}_{\mu\nu}(\omega,\boldsymbol{k})$ requires non-trivial analytic continuation to real space. Thereby, results for *momentum-dependent* real time correlators from other QCD-like strongly coupled thermal systems would be helpful.

[1] Strictly speaking, due to the symmetry $(G^{\rm R}_{\mu\nu}(\omega,\boldsymbol{k}))^* = G^{\rm R}_{\mu\nu}(-\omega^*,\boldsymbol{k})$, if $\Omega_{J/\psi}$ is a pole of $G^{\rm R}_{\mu\nu}(\omega,\boldsymbol{k})$, so is $-\Omega^*_{J/\psi}$. For definiteness, we specify $\Omega_{J/\psi}$ as the one whose real part is positive.

AdS/CFT correspondence or gauge/gravity duality [18] provides a new theoretical tool for modeling strongly-coupled thermal media. In particular, various properties of QCD, both in vacuum and at finite temperature, have been modeled within that framework (for a review, see Ref. [19] and references therein). These techniques have been applied to charmonium moving in medium previously, though they were typically from a "top-down" approach [20–22] [2]. Their results can be characterized by observing a decrease in the dissociation temperature with momentum and dispersion relation which exhibits a subluminal group velocity at asymptotically large momentum $|\boldsymbol{k}|$. However, as argued elsewhere [25], these models do not reproduce the vacuum charmonium phenomenology exceptionally well, particularly with the excited states. Therefore, it is useful to reexamine this problem with a more realistic holographic model.

In this paper, we present results on in-medium properties of moving charmonium in both transverse and longitudinal channel from the phenomenological ("bottom-up") holography model constructed in Ref. [25]. Compared with previous holographic models of heavy quarkonia (see, for example, Refs. [21, 22, 24]), this model has the advantage of capturing QCD charmonium spectral data in vacuum. Therefore, it is an ideal tool to explore the properties of charmonium at finite temperature and finite momentum.

This paper is organized in the following manner. In Sec. II, we review the vacuum holographic model of Ref. [25]. In Sec. III, this is extended to finite temperature and momentum. We present our results in Sec. IV and discuss them in Sec. V. Finally, in Sec. VI, we conclude.

II. A REVIEW OF THE HOLOGRAPHIC MODEL OF CHARMONIUM

In this section, we review some of the key aspects of the vacuum "bottom-up" holographic model of charmonium constructed in Ref. [25], and extend it to finite momentum. According to the holographic dictionary, the conserved heavy quark vector current operator $J^\mu = \bar{c}\gamma^\mu c$ is dual to a $U(1)$ gauge field V_μ on the five-dimensional asymptotic AdS_5 background. The relevant part of the bulk action has the usual Maxwell form [26, 27]:

$$S = -\frac{1}{4g_5^2}\int d^5x\sqrt{g}e^{-\phi}V_{MN}V^{MN} \tag{1}$$

[2] See also Ref. [23] for a similar "top-down" approach for mesons in general and Ref. [24] for a comparable "bottom-up" description.

where g_5^2 is the 5D gauge coupling, ϕ is the background scalar field which, in general, is a combination of dilaton and/or tachyon fields, corresponding to the conformal and/or chiral symmetry breaking, and $V_{MN} = \partial_M V_N - \partial_N V_M$. The most general metric (up to coordinate transformations) possessing three-dimensional (3D) Euclidean isometry reads

$$ds^2 = e^{2A(z)} \left(dt^2 - d\boldsymbol{x}^2 - dz^2 \right) , \tag{2}$$

where z denotes the coordinates in the fifth dimension. The gauge field can be factorized such that

$$V_M(z, \boldsymbol{x}, t) = V_M(z) e^{i\boldsymbol{k}\cdot\boldsymbol{x} - i\omega t} . \tag{3}$$

The equation of motion in $V_5 = 0$ gauge reads

$$\partial_z \left[e^{B(z)} \partial_z V \right] + (\omega^2 - \boldsymbol{k}^2) \, e^{B(z)} V = 0 , \tag{4}$$

where V is any of the three spatial components of $V_\mu(z)$, and $B(z) = A(z) - \Phi(z)$. Near the boundary $z \to 0$, $B(z)$ should behavior as $B(z) \to -\log z$ to represent asymptotic AdS_5 geometry. Via a Liouville transformation

$$\Psi = e^{B(z)/2} V , \tag{5}$$

Equation. (4) can be brought into the form of a Schrödinger equation:

$$-\frac{d^2\Psi}{dz^2} + U(z)\Psi = (\omega^2 - \boldsymbol{k}^2)\Psi , \tag{6}$$

with the "holographic potential" given by

$$U(z) = \frac{B''(z)}{2} + \left(\frac{B'(z)}{2} \right)^2 . \tag{7}$$

Here and hereafter a prime denotes the derivative with respect to z.

For the case when charmonium is at rest, $\boldsymbol{k} = 0$, discrete values of $\omega^2 = m_n^2$, for which the Eq. (6) possesses normalized bound states Ψ_n, correspond to the masses m_n of the charmonium states, $n = 1, 2, \ldots = J/\psi, \psi', \ldots$. Holographic correspondence also relates decay constants of the charmonium states to the (second) derivative of the normalized bound states $\Psi_n(z)$ (see, for example, Refs. [26, 28]):

$$f_n = \frac{1}{g_5 m_n} \left(\sqrt{z} \, \Psi_n(z) \right)'' \Big|_{z \to 0} . \tag{8}$$

In the spirit of the "bottom-up" approach, this model chooses the function $B(z)$ so as to satisfy the spectroscopic data associated with charmonium. It is assumed that such a background arises dynamically, but no attempt to model the corresponding dynamics is made. To this end, $B(z)$ is chosen such that holographic potential, Eq. (7), reads:

$$U(z) = \frac{3}{4z^2}\,\theta(z_d - z) + \left((a^2 z)^2 + c^2\right)\theta(z - z_d) - \alpha\,\delta(z - z_d)\,. \tag{9}$$

The holographic potential in Eq. (9) uses a soft-wall model, [27], for large z which successfully describes light mesons, and adds to it a "shift term," c^2, which accounts for the mass of J/ψ and a delta function "dip" to account for the relatively large J/ψ decay constant. This model will be henceforth referred to as the "shift and dip" model. In Ref. [25], the four parameters in this potential have been determined by requiring that the model correctly reproduce the masses and decay constants of J/ψ and ψ' yielding

$$\begin{aligned} &a = 0.970 \text{ GeV},\ c = 2.781 \text{ GeV}, \\ &\alpha = 1.876 \text{ GeV},\ z_d^{-1} = 2.211 \text{ GeV}\,. \end{aligned} \tag{10}$$

With this choice for $U(z)$, the function $B(z)$ can be determined from Eq. (7). For non-zero momentum, $\boldsymbol{k} \neq 0$, the gauge field can be determined by solving Eq. (6) with the same holographic potential $U(z)$ with identical parameters as the case when charmonium is at rest.

Prior to the "shift and dip" model, heavy quarkonia had been studied in the framework of gauge/gravity duality from both "top-down" approach [21, 22] and "bottom-up" approach [24]. One crucial difference between holographic models mentioned above and the "shift and dip" model is the spectrum of heavy quarkonium. In both classes of models previously considered, there is only one scale which sets the masses of both the ground state and the excited states, thus $m_n \sim n m_1$, $n \geq 1$. In contrast, in the heavy quark limit of QCD, the mass of the ground state, J/ψ, is controlled by one parameter (the heavy quark mass) which is different from the parameter (string tension, or $\Lambda_{\rm QCD}$) controlling the level spacing of excited states: $m_n^2 \sim m_1^2 + (n-1)\,\Lambda_{\rm QCD}^2$. Roughly speaking, these two scales are represented in the "shift and dip" model by the parameters c and a, respectively.

It is reasonable to expect that reproducing the charmonium spectral data, such as masses and decay constants in vacuum, is an important prerequisite for modeling behavior of charmonium at finite temperature. Therefore we choose the "shift and dip" model, which mimics

QCD charmonium at zero temperature, as a basic tool to explore in-medium properties of charmonium. As a non-trivial test of the "shift and dip" model, one of us (P.H.) has applied the heavy-quark QCD sum rules to this model [29]. There is strong agreement between the moments of the polarization function calculated from the "shift and dip" model and the experimental data, suggesting that the "shift and dip" model is consistent with the heavy-quark QCD sum rules at zero temperature. Explicit consistency checks of finite temperature QCD sum rules have not been made.

III. THERMAL CORRELATORS FROM HOLOGRAPHY

At non-zero temperatures, gauge plus rotation invariance requires that the retarded Green's function $G^{\rm R}_{\mu\nu}(\omega, \boldsymbol{k})$ has the form

$$G^{\rm R}_{\mu\nu}(\omega, \boldsymbol{k}) = P^T_{\mu\nu}(\omega, \boldsymbol{k})\, \Pi^T(\omega, \boldsymbol{k}) + P^L_{\mu\nu}(\omega, \boldsymbol{k})\, \Pi^L(\omega, \boldsymbol{k})\,, \tag{11}$$

for four momentum $k^\mu = (\omega, \boldsymbol{k})$. The transverse and the longitudinal projectors are defined in the standard way as $P^T_{00} = 0$, $P^T_{0i} = 0$, $P^T_{ij} = \delta_{ij} - k_i k_j/k^2$, and $P^L_{\mu\nu} \equiv k_\mu k_\nu/(k^\mu k_{\mu)} - g_{\mu\nu} - P^T_{\mu\nu}$, where i, j are spatial indices and $k \equiv |\boldsymbol{k}|$. $\Pi^T(\omega, k), \Pi^L(\omega, k)$ are the transverse and longitudinal correlators respectively. In the present paper, we are using the mostly minus signature as indicated by Eq. (2). The imaginary parts of $\Pi_{T,L}$ are related, by definition, to transverse and longitudinal spectral functions:

$$\rho_{T,L}(\omega, k) = -{\rm Im}\Pi_{T,L}(\omega, k). \tag{12}$$

To study $\rho_{T,L}(\omega, k)$ from holography at finite temperature, a blackhole ansatz for the metric is chosen:

$$ds^2 = e^{2A(z)} \left(h dt^2 - d\boldsymbol{x}^2 - h^{-1} dz^2 \right). \tag{13}$$

If the function $h(z)$ has a simple zero, *viz.* $h(z_h) = 0$, the space described by (13) possesses a horizon at $z = z_h$. The temperature T corresponding to this background is related to z_h as

$$T = \frac{1}{4\pi} \left| h'(z_h) \right| \ . \tag{14}$$

We assume the simplest ansatz for h, namely,

$$h(z) = 1 - (z/z_h)^4\,, \tag{15}$$

which turns out to be the same as that in the familiar AdS_5 blackhole solution. The temperature T corresponding to this background is related to z_h as $z_h = (\pi T)^{-1}$. In principle, we should expect the function $A(z)$ as well as the background $\Phi(z)$ to depend on the temperature. Since we do not attempt to model the background dynamically even at zero temperature, we will use the simplest form of temperature dependence as it is conventionally assumed when studying temperature-dependent quantities in "bottom-up" models (see e.g. Refs. [24, 25, 30]).

With the metric in Eq. (13), the transverse and longitudinal fluctuations, V_T and V_L, at finite momentum k satisfy the equations:

$$V_T''(z) + \left(B'(z) + \frac{h'(z)}{h(z)} \right) V_T'(z) + \frac{\omega^2 - k^2 h(z)}{h^2(z)} V_T(z) = 0\,, \tag{16a}$$

$$V_L''(z) + \left(B'(z) + \frac{\omega^2}{(\omega^2 - k^2 h(z))} \frac{h'(z)}{h(z)} \right) V_L'(z) + \frac{\omega^2 - k^2 h(z)}{h^2(z)} V_L(z) = 0\,. \tag{16b}$$

At zero momentum, Eqs. (16a) and (16b) are identical as expected. $\Pi_{T,L}(\omega, k)$ can be calculated according to standard holographic prescriptions [31]:

$$\Pi_{T,L}(\omega, k) = -\frac{1}{g_5^2}\, h e^B \frac{V_{T,L}'(z,\omega,k)}{V_{T,L}(z,\omega,k)}\bigg|_{z=\epsilon} = -\frac{1}{g_5^2}\, \frac{V_{T,L}'(\epsilon,\omega,k)}{\epsilon V_{T,L}(\epsilon,\omega,k)}, \tag{17}$$

where $\epsilon \to 0$ is an ultraviolet regulator and $V(z,\omega,k)$ is the solution to Eq. (16) satisfying infalling wave boundary conditions near the horizon:

$$V(z,\omega,k) \xrightarrow{z \to z_h} (1 - z/z_h)^{-i\omega/(4\pi T)}\,. \tag{18}$$

Equation (16) with the boundary condition of Eq. (18) must be solved numerically in the present model. The longitudinal equation Eq. (16b) is slightly more subtle as it will have an integrable singularity if $\omega^2 - k^2 h(z)$ has a root between the boundary and the horizon for fixed ω and k. However, this singularity may be avoided by making an infinitesimal Wick rotation as pointed out in Ref. [32].

At finite temperature, it is also useful to apply the Liouville transformation

$$\Psi(\xi(z)) = e^{B(z)/2} V_T(z)\,, \qquad \xi(z) = \int_0^z \frac{dz'}{h(z')} \tag{19}$$

to the transverse equation of motion Eq. (16a). In the new coordinate ξ, we arrive at a "Schrödinger" equation:

$$\frac{d^2\Psi}{d\xi^2} + \left[(\omega^2 - k^2) - U_{\rm sch}(\xi, k) \right] \Psi = 0\,, \tag{20}$$

with the finite temperature "holographic potential" given by

$$U_{\rm sch}(\xi(z),k) = h(z)^2\left[\frac{B''(z)}{2}+\left(\frac{B'(z)}{2}\right)^2+\frac{B'(z)h'(z)}{2h(z)}\right]-k^2z^4\,. \tag{21}$$

A similar prescription is not as useful for the longitudinal equation of motion because the resulting Schrödinger coordinate and Schrödinger potential are in general complex.

IV. J/ψ MOVING IN A STRONGLY COUPLED PLASMA

A. Rescaled spectral functions

It is convenient to define a dimensionless rescaled spectral density [25]:

$$\bar{\rho}_{T,L}(\omega,k) \equiv \frac{[\rho_{T,L}(\omega,k)/\omega^2]}{[\rho_{T,L}(\omega,0)/\omega^2]\,|_{\omega\to\infty}} = \frac{2g_5^2}{\pi}\frac{\rho(\omega,k)}{\omega^2} \tag{22}$$

such that $\bar{\rho}_{T,L}(\omega\to\infty,k)=1$. Here we have used the fact that in large ω limit, $\rho_{T,L}(\omega,k)/\omega^2$ will approach its zero temperature limit $\pi/2g_5^2$ for any finite k.

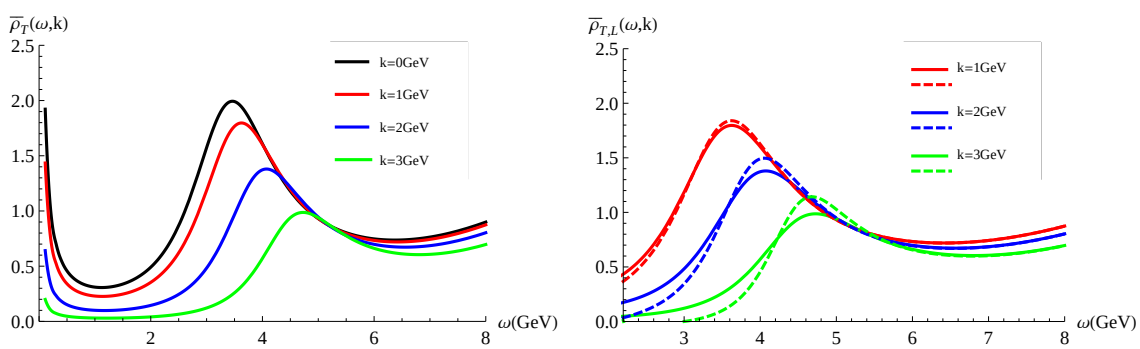

(a) (b)

FIG. 1. Left: Rescaled spectral functions in transverse channel, $\bar{\rho}_T(\omega,k)$, defined by Eq. (22) at $T=0.74\,T_{\rm D}(k=0)$ where $T_{\rm D}(k=0)$ is the dissociation temperature at zero momentum. Black, red, blue and green curves are corresponding to $k=0,1,2,3$ GeV, respectively. Right: Comparison between rescaled spectral functions, $\bar{\rho}(\omega,k)$, in transverse channel (solid) and longitudinal channel (dashed) at $T=0.74\,T_{\rm D}(k=0)$. Red, blue and green curves correspond to momenta $k=1,2,3$ GeV in each channel.

Figure 1(a) plots the rescaled spectral functions $\bar{\rho}_T(\omega,k)$ from the "shift and dip" model in the transverse channel at $T=0.74\,T_{\rm D}(k=0)$ where $T_{\rm D}(k=0)$ is the J/ψ dissociation

temperature at zero momentum (cf. Sec. IV C below or Ref. [25] for the discussions on determination of $T_{\rm D}(k=0)$). We first observe that the ψ' has already merged into the continuum even at zero momentum. Thus further discussions on ψ' at finite momentum will not be made. Secondly, the peak location corresponding to the J/ψ metastable state moves to larger ω while the peak height is attenuated as momentum increases. The sharp peak at $\omega = 0$ in the transverse channel is associated with the conductivity of the current of charm charge when $k = 0$. At finite k, this peak, i.e., $\rho(\omega, k)/\omega$, decreases with increasing momentum.

To compare the transverse and longitudinal spectral functions, we plot $\bar{\rho}_T(\omega, k)$ and $\bar{\rho}_L(\omega, k)$ in Fig. 1(b) at $T = 0.74\, T_{\rm D}(k = 0)$ for $k = 1, 2, 3$ GeV. For frequencies around and larger than the peak region, the transverse and longitudinal spectral functions are quite similar. In the peak region, the shift in mass with momentum is also similar between the two modes. The height of the peak is less attenuated while it is narrower in the longitudinal mode compared with the transverse mode.

B. Dispersion relation and spectral width

To quantify the properties of the spectral function, we can calculate the poles of the retarded Green's function, denoted by $\Omega_{T,L}(k, T)$. On the field theory side, the real part of the pole is attributed to the peak mass while the negative of the imaginary part with the width. In the literature of holographic correspondence, those poles are referred to as quasi-normal modes [33] which can be determined by solving $V(\epsilon, \Omega, k) = 0$, using the solutions of Eq. (16) and boundary conditions given in Eq. (18) for any given k. At zero temperature and zero momentum, $\Omega_T(k = 0, T = 0) = \Omega_L(k = 0, T = 0) = M_{J/\psi}$. We will present numerically determined $\Omega_{T,L}(k, T)$ below.

Figure 2 plots the pole mass of J/ψ, $\mathrm{Re}\,\Omega_{T,L}(k, T)$, as a function of momentum. These curves represent the in-medium dispersion relation of J/ψ calculated from the "shift and dip" model. They are plotted at three different temperatures, from bottom to top, $T = 200$ MeV (red), $T = 300$ MeV (blue), and $T = 400$ MeV (green). The dispersion relation shows little temperature dependence and no indication of a subluminal limiting velocity. Moreover, the transverse and longitudinal modes reveal nearly identical dispersion relations. This is consistent with our results on spectral densities presented in last section(cf. Fig. 1(b)).

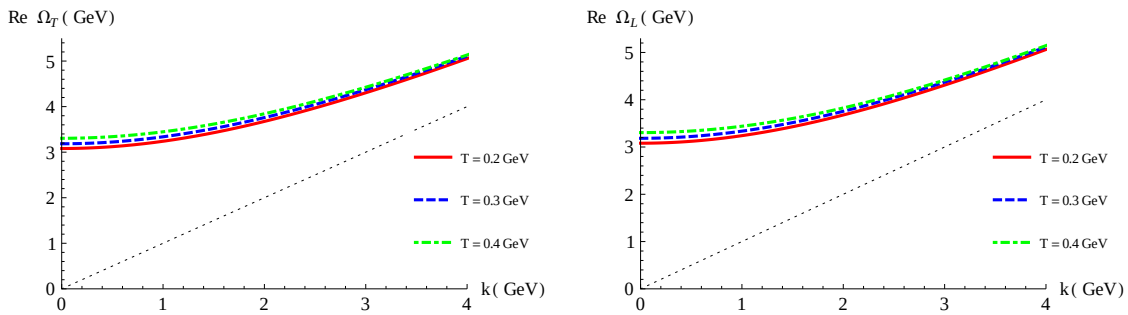

(a) (b)

FIG. 2. Left: Dispersion relation for J/ψ in the transverse channel. Right: Dispersion relation for J/ψ in longitudinal channel. Red,blue and green curves are corresponding to $T = 200, 300, 400$ MeV respectively. The dotted curve is corresponding to the light cone.

Numerically, the relative difference between $\Omega_T(k,T)$ and $\Omega_L(k,T)$ at fixed k, T is within a few percent for all temperatures above T_c and momenta which we are considering.

The quasinormal modes can also be used to determine the peak width of J/ψ: $\Gamma_{L,T} = -\mathrm{Im}\Omega_{L,T}$. Figure 3(a) presents the width $\Gamma_{L,T}(k,T)$ as a function of momentum for four different temperatures for both transverse and longitudinal channel. In the transverse channel,

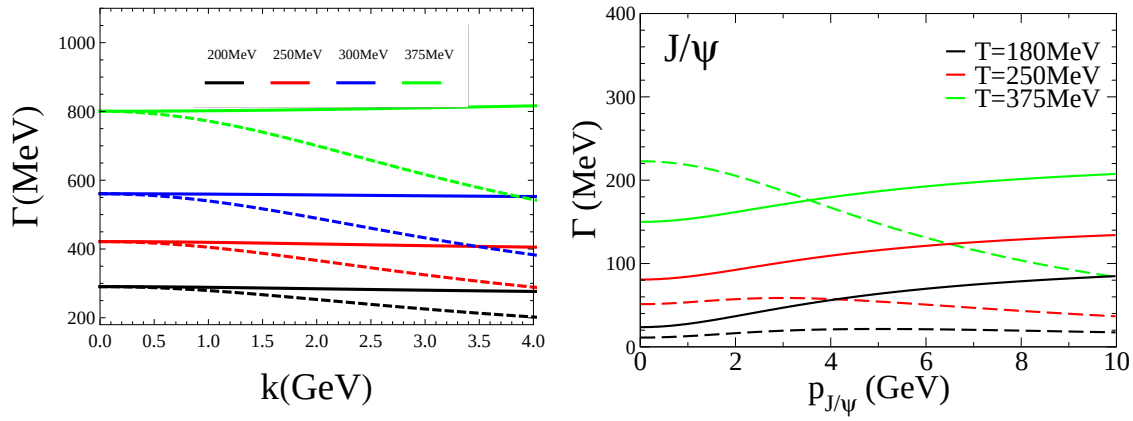

(a) (b)

FIG. 3. Left: Momentum dependence of the total width of J/ψ in transverse channel. Black,red, blue and green curves are corresponding to $T = 200, 250, 300, 375$ MeV respectively. Dashed curves are corresponding to those from the longitudinal channel. Right: Momentum dependence of quasi-free (solid line) and gluo-dissociation rates (dashed line) for J/ψ calculated from perturbative QCD at different temperatures from Ref. [34] (see also Ref. [6]).

the width is a slowly varying function of momentum for all temperatures we are considering. On the other hand, the width will decrease as momentum increases in the longitudinal channel. This numerical behavior is consistent with the qualitative observations from the last section.

C. Momentum dependence of the dissociation temperature

We now study the momentum dependence of the dissociation temperature. In order to determine the dissociation temperature, T_D, of J/ψ, one must select a criteria. In general, T_D is associated with the temperature when the J/ψ peak is no longer present in the spectral function. Yet a more specific criteria is useful. We will follow Ref. [25] and define the dissociation temperature $T_D(k)$ at momentum k as the temperature below which the height of the J/ψ peak, $H_{J/\psi}$, of the rescaled spectral functions $\bar{\rho}(\omega, k)$ is smaller than some threshold value, say H_D. Of course, there is no unique choice of H_D, similar to the situation that there is no precise definition of screening length below which J/ψ will dissociate. In Ref. [25], the simplest criterion

$$H_D = 1 \tag{23}$$

is used to quantify the dissociation temperature. The idea behind this criterion is that a J/ψ state can be considered as being merged into continuum if its peak is lower than the asymptotic value of the rescaled spectral function $\bar{\rho}(\omega, k)$, and thus be considered dissociated. We will follow the criterion of Eq. (23) here. It should be also pointed out that the peak height calculated in the present holographic model is a monotonic function of both momentum and temperature, which makes it suitable as a criterion candidate. At zero momentum, the rescaled spectral density calculated from "shift and dip" model $\bar{\rho}(\omega, k = 0)$ supports a J/ψ peak up to at least 500 MeV [25]. Using the criterion in Eq. (23), the zero momentum dissociation temperature is found to be

$$T_{\rm D}(k = 0) = 540\,{\rm MeV}\,. \tag{24}$$

This is consistent with lattice measurements reported in Refs. [10, 11] that J/ψ will survive up to $2 \sim 2.4\,T_c$ with $T_c = 190$ MeV but is higher than the lattice results of Ref. [12] that J/ψ are found to dissociate already at $1.5\,T_c$.

Using this selection process, T_D can be determined as as a function of momentum. This is plotted in Fig. 4(a). Observe that, as expected, as momentum increases, the dissociation temperature decreases. Furthermore, the transverse mode decreases faster than the longitudinal mode with momentum. This is in accordance to the difference in the peak height of the spectral functions seen above. At a finite momenta, the dissociation temperature becomes equal to T_c. Though there is no manifestly inherent transition in this model at this momentum, on physical grounds T_D should be greater than T_c. One can also ask the question, for a given temperature, what is the largest momentum J/ψ could have before it dissociates. This limiting momentum, $k_{\rm lim}$, is shown in Fig. 4(b). The maximum value $k_{\rm lim}$ can achieve is at $T = T_c$, *i.e.* when $T_D(k_{\rm lim}^{\rm max}) = T_c$. This condition suggests that the momentum of charmonia in-medium could be limited to a maximum value unrelated to any dispersion relation. For $T_c \sim 190$ MeV, we find the maximum momentum to be $k_{\rm lim}^{\rm max} = 3.8$ GeV for the transverse mode and $k_{\rm lim}^{\rm max} = 4.2$ GeV for the longitudinal mode. The implications of this momentum will be discussed in subsequent sections.

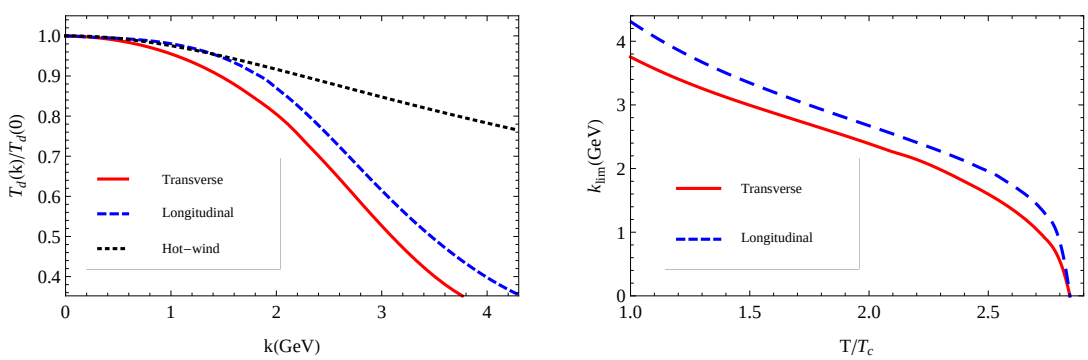

(a) (b)

FIG. 4. Left panel: Momentum dependence of the dissociation temperature $T_{\rm D}(k)/T_{\rm D}(k=0)$ in the range $T_{\rm D}(k=0) \geq T_{\rm D}(k) \geq T_{\rm c}$ in the transverse channel (red, solid) and the longitudinal channel (blue, dashed) with $T_c = 190$ MeV. The dotted curve shows the momentum dependence of the dissociation temperature based on the holographic analysis of color screening length [20] assuming the approximate scaling in Eq. (28) and a relativistic on-shell relation. Right panel: The limiting momentum $k_{\rm lim}$ as a function of temperature T in the transverse (red) and the longitudinal (blue) channels with $T_c = 190$ MeV.

V. DISCUSSION

In this section, we will interpret and discuss the results which were represented in the previous sections, while also placing them in the context of existing literature.

A. J/ψ peak height

The most important result presented in this paper is the decrease in dissociation temperature with momentum. This momentum dependence is due to the decrease of the height of the J/ψ peak in both the transverse and longitudinal modes. This behavior is qualitativley in agreement with results from lattice [12], holography [21, 22, 35] and heavy quark effective theory [7]. Moreover, the height of the J/ψ peak is related to the width Γ and the (rescaled) residue associated with J/ψ pole of $G^{\mathrm{R}}_{\mu\nu}(\omega, \boldsymbol{k})$, i.e. ,

$$H \equiv \frac{\mathrm{Re}\,(r_{J/\psi})}{\Gamma}\,. \tag{25}$$

Here the rescaled residue $r_{J/\psi}$ corresponding to the J/ψ pole is defined by

$$r_{J/\psi} \equiv \frac{2g_5^2}{\pi\,\Omega^2_{J/\psi}} \lim_{\omega\to\Omega_{J/\psi}} \big(\omega - \Omega_{J/\psi}(k)\big)\,\Pi^{\mathrm{T,L}}(\omega, k)\,. \tag{26}$$

It is interesting to identify whether the momentum dependence of the height is associated with the width or the residue. In holographic models, the width Γ and the rescaled residue $r_{J/\psi}$ can be easily calculated. The momentum dependence of Γ and $r_{J/\psi}$ are ploted in Figs. 3(a) and 5(a) respectively. Comparing those figures with the momentum dependence of J/ψ peak height H in Fig. 5(b), we found that in the present model, the momentum dependence of J/ψ peak height H is dominated by the momentum dependence of the rescaled residue $r_{J/\psi}$. Indeed, in transverse channel, the width is a slowly varying function of k while in the longitudinal channel, the width even decreases with growing momentum. However, due to relatively rapid decreasing of the rescaled residue $r_{J/\psi}$, the height H is attenuated in both channels. Therefore we must conclude that the dissociation temperature is more sensitive to the residue rather than the width of the peak.

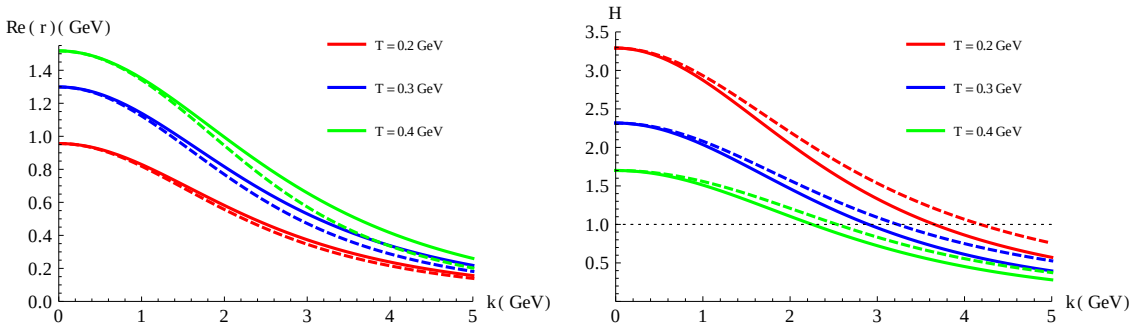

(a) (b)

FIG. 5. Left: Momentum dependence of the real part of the residue of J/ψ in transverse channel. Red,blue and green curves are corresponding to $T = 200, 300, 400$ MeV respectively. Dashed curves are corresponding to those from the longitudinal channel. Right: Momentum dependence of the height of J/ψ in transverse channel. Red, blue and green curves are corresponding to $T = 200, 300, 400$ MeV respectively. Dashed curves are corresponding to those from the longitudinal channel.

B. Total width

One striking result was the different behaviors of the J/ψ width between the transverse and longitudinal channels. One can understand the behavior of J/ψ width in the transverse channel shown in Fig. 3(a) from the gravity side of the duality. The finite temperature and momentum state corresponding to charmonium is represented by a metastable quantum state which satisfies an equation of Schrödinger form, Eq. (20), with the holographic potential Eq. (21). Therefore, one can apply one's normal intuition concerning quantum mechanical systems. In Fig. 6, the holographic Schrödinger potential is plotted at $T = 400$ MeV and a variety of momenta. One can clearly see that the potential barrier at higher values of ξ, the "Schödinger coordinate" defined in Eq. (19), decreases in magnitude and narrows with momentum. Therefore, at higher momentum, it is easier for the quantum state to tunnel through this barrier and thus decay. Consequently, the absolute value of the imaginary part of $(\Omega_{J/\psi})^2$, $2(Re\Omega_{J/\psi})\Gamma$, will increase with higher momentum. On the other hand, as we see from Fig. 2(a), $Re\Omega_{J/\psi}$ is also growing with increasing momentum. As a result, the change of the total width, Γ, in transverse channel is relatively slow. Unfortunately, a similar argument for the longitudinal mode is not as clean because both the Schrödinger

potential and its coordinate are complex. However, the different behaviors of the J/ψ width may be understood as a "Doppler-like" effect analogous to that seen in the weakly coupled calculation of Ref. [7]. The difference between the two channels may also imply a coupling between the spin and the gluon fields on the field theory side.

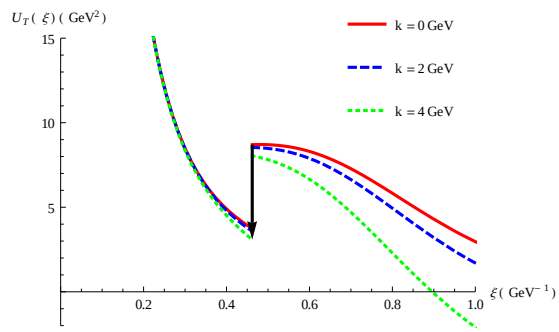

FIG. 6. Holographic potential Eq. (20) at $T = 400$ GeV with $k = 0$ GeV (red,solid), $k = 2$ GeV (blue,dashed), $k = 4$ GeV (green, dotted) respectively. The black arrow indicates the negative delta-function in "holographic potential" at $z = z_d$.

The numerical results for the peak width as a function of momentum can also be compared with the expectations from QCD. In the QGP, J/ψ may be (inelastically) dissociated via either interactions with gluons, i.e. gluon dissociation reactions, $J/\psi + g \to c + \bar{c}$, or collisions with partons in the medium, i.e. quasi-free dissociation, $X + J/\psi \to X + c + \bar{c}(X = g, q, \bar{q})$ [6, 34]. These two mechanisms have different momentum dependence. Due to increasing color screening length, gluon dissociation tends to be a decreasing function of momentum. On the other hand, the quasi-free dissociation rate always increases with momentum due to a smoothly increasing cross section with increasing center-of-mass energy. The momentum dependence of each of these process has been previously calculated in Ref. [34] and illustrated in Fig. 3(b). The combination of the two process results in a width which increases with momentum at lower temperatures and decreases with momentum at higher temperatures. If we average over the polarization states in the holographic model, we observe a qualitative similar trend, that as one increases the temperature, the width decreases more and more with momentum because of the behavior of the longitudinal channel. The absolute size of the width for the current model is larger than the QCD predictions, but this may be because the holographic width includes both inelastic and elastic scattering whereas the

QCD width only includes the former. Nevertheless, it is interesting to note the qualitative similar momentum behavior between strongly and weakly coupled calculation.

C. Lattice

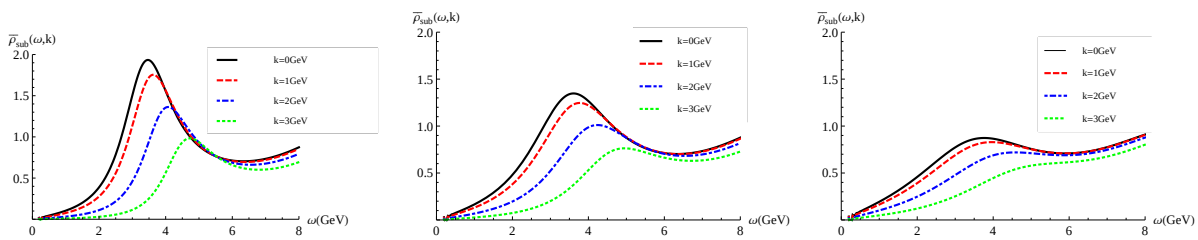

(a) (b) (c)

FIG. 7. Momentum dependence of $\bar{\rho}_{\rm sub}(\omega, k)$ defined by Eq. (27) at $T = 0.74\,T_{\rm D}(k = 0)$(left), $T = 0.94\,T_{\rm D}(k = 0)$(middle) and $T = 1.1\,T_{\rm D}(k = 0)$(right). Black, red, blue and green curves are corresponding to $k = 0, 1, 2, 3$ GeV respectively.

One motivation of the present paper is to provide complementary information for the lattice measurement of J/ψ spectral function. One may note that as the width of the transport peak is inversely proportional to the mean free path, spectral functions calculated from holography generically will have a relatively broadened hydrodynamic peak. To minimize the effects of such broadened transport peaks on the J/ψ peaks we are interested in and to make a closer comparison with lattice results, we define a subtracted rescaled spectral function,

$$\bar{\rho}_{\rm sub}(\omega, k) = \bar{\rho}(\omega, k) - \frac{1}{\omega} \lim_{\omega \to 0} \left[\rho(\omega, k)/\omega\right] . \tag{27}$$

At zero momentum, $\bar{\rho}_{\rm sub}(\omega, 0)$ is just the rescaled spectral function with the subtraction of the transport peak[3]. We plot $\bar{\rho}_{\rm sub}(\omega, k)$ in the transverse channel for three representative temperatures $T = 0.74, 0.94, 1.1\,T_{\rm D}(k = 0)$ in Fig. 7. As we have mentioned earlier in Sec. IV C, there is a discrepancy in zero momentum dissociation temperature $T_{\rm D}(k = 0)$ between the holographic calculations and the lattice literature. To minimize the ambiguities due to the difference in $T_{\rm D}(k = 0)$ and to highlight the momentum dependency, results

[3] The definition of $\bar{\rho}_{\rm sub}(\omega, k)$ in Eq. (27) is motivated by a sum-rule type model-independent relation which holds for a large class of field theories with a generic gravity dual description that spectral functions can be represented as a *convergent* sum over simple poles of the corresponding retarded Green's function in terms of conductivity σ and the residues [36].

presented in Fig. 7 should be compared with existing and future lattice measurements at the same temperature relative to the zero momentum dissociation temperature, i.e., $T/T_{\rm D}(k = 0)$. Specifically, the transverse spectral density measured at $T = 1.46T_c$ on the lattice by Ref. [16],see Fig. 8, should be compared with the holographic calculation at $T = 1.1T_D(k = 0)$, i.e., Fig. 7(c). Furthermore, the different behavior of the transverse and longitudinal channels observed here is qualitatively confirmed by the lattice calculations of Ref. [14].

Indeed, the momentum dependence of spectral density from the "shift and dip" model at that relative temperature is qualitatively consistent with the lattice reconstructed spectral function reported recently in Ref. [16](see also Fig. 8). We take this agreement as one of the evidences that the "shift and dip" model is consistent with the in-medium properties of charmonium.

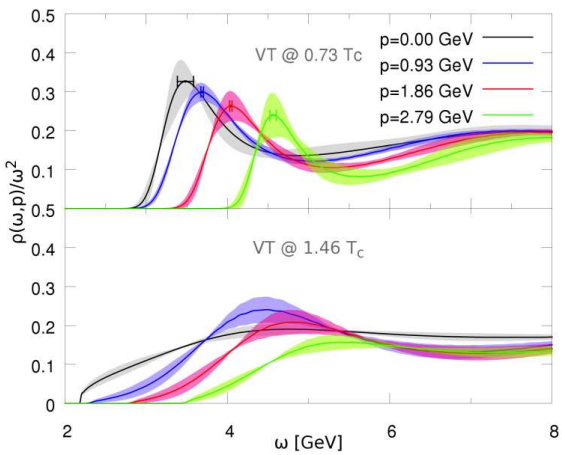

FIG. 8. Lattice measurements of momentum-dependent (rescaled) spectral functions in transverse channel in Ref. [16] .

D. Limiting velocity

The dispersion relation results indicate little temperature dependence and no indication of a subluminal limiting velocity, i.e., $\omega \sim v_g k$ with $v_g = 1$ for large k. This is consistent with the analysis of Ref. [37] which used a WKB approximation to determine the dispersion relation for large k in a class of holographic models. However, it is contrary to the work of [22] which was based on a "top-down" perspective, and treated charmonium as an excitation of a D-branes. There they found that although for large k, $\omega \sim v_g k$, v_g depends on the

temperature and is smaller than 1. The observation of a subluminal limiting velocity in "top-down" models was also established in Ref. [21]. It was suggested that the presence of this subluminal limiting velocity was associated with charmonium melting, i.e., if the group velocity of a J/ψ were greater than that subluminal group velocity, it would dissociate. Moreover, as noticed in Ref. [38], if dispersion relation curve of the heavy quarkonia crosses the light-cone at some point in the frequency space, photon production rate per energy will have a peak accordingly. Based on the above observations and generic features of dispersion relation of quarkonia found in "top-down" holographic approach [21, 22], authors of Ref. [38] predicted a photon production peak between 3 and 5 GeV due to J/ψ in heavy ion collisions.

We can understand the discrepancy between these other models and the results presented here in the following way. In each of the "top-down" constructions in Refs. [21, 22], D-branes lie completely outside the horizon in a "Minkowski embedding." In the large k limit, the wave function of a meson is localized at the tip of the branes. Consequently, the limiting group velocity of this meson approaches the local speed of light at the tip of the branes and is subluminal compared with the speed of light in flat space. For the class of models including the "shift and dip" model, the bulk geometry extends to the horizon. As conjectured in Ref. [39] and shown in Ref. [37] via WKB analysis, in such geometries, the support of quasinormal modes becomes increasingly focused at the asymptotic AdS boundary, where the local speed of light is asymptotically 1. Thus the limiting group velocity is 1 as well. Furthermore, because the dispersion relation of the current model does not cross the light cone, we would not expect to observe a peak in the photon production due to J/ψ. This is then consistent with the recent experimental report [40] on photon production with Au-Au collision at $\sqrt{s_{NN}} = 200$ GeV by the PHENIX collaboration. This suggests that in the future holographic constructions, certain constraints from experiment on limiting velocity should be taken into account.

E. Hot wind

Next we come to the dissociation temperature as a function of momentum. In the pioneering work of Ref. [20], the Wilson loop, thus the heavy quark effective potential, and the color screening length in a "hot wind" have been calculated using holographic techniques. The authors of Ref. [20] found that the dissociation temperature T_D, defined as the temper-

ature such that the screening length is the same order as the size of the quarkonia, decreases as the relative velocity v_r between the heavy quarkonia and the medium increases. To good accuracy, the dissociation temperature scales with relative velocity v_r as:

$$T_D(v_r) \approx (1 - v_r^2)^{1/4} T_D(v_r = 0)\,. \tag{28}$$

The scaling behavior of Eq. (28) may be understood from relativistic kinematics [19]. Considering a meson moving through the plasma with velocity v_r, it experiences a higher energy density, boosted by a factor of $\gamma^2 = (1 - v_r^2)^{-1}$. As energy density is proportional to T^4, the effective temperature is boosted by a factor of $\sqrt{\gamma} = (1 - v_r^2)^{-1/4}$. This parallels the previous observation that the limiting velocity of Refs. [21, 22] had the same dependence on temperature as the dissociation temperature for the "hot-wind" model had on momentum.

For the sake of the comparison, we convert Eq. (28) into the momentum dependence of $T_D(k)$ assuming relativistic kinematic relation $\omega(k) = \sqrt{k^2 + M_{J/\psi}^2}$ and plot $T_D(k)$ verses k in Fig. 4(a) (dotted line, see also Fig. 3 of Ref. [20]). Qualitatively, we see from Fig. 4(a) that the dissociation temperature T_D determined either from the screening length or the height of J/ψ peak is a decreasing function of momentum with the present approach decreasing faster than the "hot wind" analysis. This difference may be attributed to the fact that in addition to color screening, other dissociation mechanisms such as thermal broadening, are also incorporated in the current study. The present analysis on dissociation temperature provides new insights, which are complementary to previous ones, into the momentum dependence of J/ψ dissociation.

F. Nuclear modification factor, R_{AA}, and a maximum momentum

Throughout this paper, we have calculated the attenuation of J/ψ peak height with increasing momentum and determined the dissociation temperature $T_{\rm D}(k)$ as a function of J/ψ momentum k based upon height of the spectral peak. This was a convenient choice because it was a monotonic function of both temperature and momentum, and thereby removed ambiguities of selecting the dissociation temperature besides that which was associated with the criterion. Yet the relevant experimental observable for J/ψ suppression is the nuclear modification factor, R_{AA}. It is not clear *a priori* which aspect of the equilibrium properties of charmonium is most important to determine R_{AA}. For this discussion, we will focus

on the dissociation temperature. If T_D were the dominated factor in determining R_{AA}, we would speculate, from the results presented here, that R_{AA} should decrease as a function of momentum. Yet, as we have indicated above, this decrease should not continue to arbitrarily small temperatures; the dissociation temperature needs to be restricted to $T_D > T_c$. We have shown in Sec. IV C that this condition implies that there is a maximum momentum which J/ψ could achieve before dissociation, namely $k_{\rm lim}^{\rm max}$. If J/ψ is completely dissolved above this momentum, this would constitute a maximum level of suppression. Therefore, R_{AA} should decrease with increasing momentum until it approaches this maximum level of suppression at some critical momentum set by $k_{\rm lim}^{\rm max}$, and remain relatively constant after that. More precisely, that implies that (a) R_{AA} would decrease with increasing rapidity and (b) the p_t that a saturated suppression begins would also decrease with increasing rapidity. This is exactly what is observed at RHIC [2, 3].

We would also like to remind the reader that though we have emphasized throughout the differences, if any, between the transverse and longitudinal modes, this distinction is not experimentally possible at this time. Thus for any comparison with experiment one would need to average over the polarization states. The holographic model described here suggests $k_{\rm lim}^{\rm max} \sim 3-4$ GeV. Remember that this is given in the rest frame of the plasma, so in the lab frame, this would be different depending on the velocity of the expanding QGP. Additionally, in the present paper, we have been considering charmonia which are in equilibrium with the medium. This is not the only source of charmonia yields observed in experiment. Therefore our results would only apply to R_{AA} in the p_t window where the yields are dominated by those J/ψ in equilibrium with the QGP. Lastly, we have described the transition from undissociated to dissociated as being rather sharp while physically this is not the case. This would simply smear out the effect and the onset of a limiting momentum.

The momentum dependence of R_{AA} speculated here is based solely on the momentum dependence of T_D. Thus the existence of a limiting momentum is not a unique feature of "shift and dip" model. Any model whose dissociation temperature decreases monotonically with momentum would see a similar feature, including other holographic models and pQCD calculations. The difference, from the phenomenological point of view, would be the numerical value of that limiting momentum, $k_{\rm lim}^{\rm max}$. Remarkably, the limiting momentum obtained from the present model is much lower than previous holographic models [22, 35]. What is more, if we take $k_{\rm lim}^{\rm max}$ as a crude estimate of the p_t for charmonia at midrapidity then the

results obtained here are quantitatively in agreement with experiment results [2, 5] that a saturated suppression begins around $p_t = 3 \sim 4$GeV.

VI. SUMMARY

In this paper, we have studied the properties of charmonium moving in a strongly coupled medium from a holographic model. The holographic model in question reproduces the vacuum properties of charmonium which makes it a suitable candidate for the current study. Results for the spectral functions for both the transverse and longitudinal channels are reported in Figs. 1 and 7. Agreements with lattice results [16] are observed. Considering the on-going efforts on understanding momentum-dependent spectral function from lattice, our results from QCD-like strongly interacting thermal systems are timely.

Most importantly, we obtained the momentum dependence of the dissociation temperature $T_D(k)$ shown in Fig. 4(a). This is determined by studying the momentum dependence of the height of the J/ψ spectral peak. It was observed that this dependence is associated with the residue of the J/ψ pole rather than the width. We also find that the momentum dependence of the spectral width is qualitatively consistent with similar calculations from a perturbative QCD perspective. The dispersion relations for J/ψ have also been calculated and reveal no subluminal limiting velocity and show no indication of a peak in the photon production rate. Based on the dissociation temperature, we found that there would be no sharp J/ψ peak in spectral density with momentum greater than $3.8 \sim 4.2$ GeV for temperatures relevant to the experiment. Though it is too early to translate the knowledge about $T_D(k)$ into experimental observables, in particular, the nuclear modification factor, R_{AA}, the presence of a limiting momentum suggests a saturation of J/ψ suppression above some momentum. To understand which properties of the spectral peak are the best indicator of R_{AA}, simulations using phenomenological models with a realistic representation of the fireball evolution, such as kinetic rate equations, transport and statistical models (see, for example, Ref. [41] and reference therein) are required. Holographic results presented here, can, in principle, provide useful information to those simulations. This work has described many key features of charmonium phenomenology and has demonstrated the usefulness of holographic models in describing them.

ACKNOWLEDGMENTS

We would like to thank the Institute for Nuclear Theory at the University of Washington for hospitality during the INT Summer School on Applications of String Theory, when part of this work was initiated. We thank Tom Faulkner, Krishina Rajagopal for discussions on heavy quarks from "top-down" holographic models, Heng-Tong Ding for email communications on the lattice data and Misha Stephanov for commenting on the draft. Y.Y. would also like to thank Wai-Yee Keung, Ho-ung Yee and Todd Springer for fruitful discussions. The work of P.H was supported in part by US-NSF under Grant No. PHY-0969394, the work of Y.Y. in part by DOE under Grant No. DE-FG0201ER41195 and UIC dean's scholar fellowship.

---

[1] T. Matsui and H. Satz, Phys.Lett. **B178**, 416 (1986).

[2] A. Adare et al. (PHENIX Collaboration), Phys.Rev.Lett. **98**, 232301 (2007), arXiv:nucl-ex/0611020 [nucl-ex].

[3] A. Adare et al. (PHENIX Collaboration), Phys.Rev.Lett. **101**, 122301 (2008), arXiv:0801.0220 [nucl-ex].

[4] S. Chatrchyan et al. (CMS Collaboration), JHEP **1205**, 063 (2012), arXiv:1201.5069 [nucl-ex].

[5] L. Adamczyk et al. (STAR Collaboration), (2012), arXiv:1208.2736 [nucl-ex].

[6] R. Rapp, D. Blaschke, and P. Crochet, Prog.Part.Nucl.Phys. **65**, 209 (2010), arXiv:0807.2470 [hep-ph].

[7] M. A. Escobedo, J. Soto, and M. Mannarelli, Phys.Rev. **D84**, 016008 (2011), arXiv:1105.1249 [hep-ph].

[8] M. A. Escobedo, F. Giannuzzi, M. Mannarelli, and J. Soto, (2013), arXiv:1304.4087 [hep-ph].

[9] N. Brambilla, M. A. Escobedo, J. Ghiglieri, and A. Vairo, **JHEP05**, 130 (2013), arXiv:1303.6097 [hep-ph].

[10] A. Jakovac, P. Petreczky, K. Petrov, and A. Velytsky, Phys.Rev. **D75**, 014506 (2007), arXiv:hep-lat/0611017 [hep-lat].

[11] G. Aarts, C. Allton, M. B. Oktay, M. Peardon, and J.-I. Skullerud, Phys.Rev. **D76**, 094513 (2007), arXiv:0705.2198 [hep-lat].

[12] H. Ding, A. Francis, O. Kaczmarek, F. Karsch, H. Satz, et al., Phys.Rev. **D86**, 014509 (2012), arXiv:1204.4945 [hep-lat].

[13] S. Datta, F. Karsch, P. Petreczky, and I. Wetzorke, Phys. Rev. D **69**, 094507 (2004).

[14] M. B. Oktay and J.-I. Skullerud, (2010), arXiv:1005.1209 [hep-lat].

[15] C. Nonaka, M. Asakawa, M. Kitazawa, and Y. Kohno, J.Phys. **G38**, 124109 (2011).

[16] H.-T. Ding, (2012), arXiv:1210.5442 [nucl-th].

[17] G. Aarts, C. Allton, S. Kim, M. P. Lombardo, M. B. Oktay, et al., JHEP **1303**, 084 (2013), arXiv:1210.2903 [hep-lat].

[18] J. M. Maldacena, Adv. Theor. Math. Phys. **2**, 231 (1998), arXiv:hep-th/9711200; S. S. Gubser, I. R. Klebanov, and A. M. Polyakov, Phys. Lett. **B428**, 105 (1998), arXiv:hep-th/9802109; E. Witten, Adv. Theor. Math. Phys. **2**, 253 (1998), arXiv:hep-th/9802150.

[19] J. Casalderrey-Solana, H. Liu, D. Mateos, K. Rajagopal, and U. A. Wiedemann, (2011), arXiv:1101.0618 [hep-th].

[20] H. Liu, K. Rajagopal, and U. A. Wiedemann, Phys.Rev.Lett. **98**, 182301 (2007), arXiv:hep-ph/0607062 [hep-ph].

[21] D. Mateos, R. C. Myers, and R. M. Thomson, Phys.Rev.Lett. **97**, 091601 (2006), arXiv:hep-th/0605046 [hep-th].

[22] Q. J. Ejaz, T. Faulkner, H. Liu, K. Rajagopal, and U. A. Wiedemann, JHEP **0804**, 089 (2008), arXiv:0712.0590 [hep-th].

[23] T. Albash, V. G. Filev, C. V. Johnson, and A. Kundu, Phys.Rev. **D77**, 066004 (2008), arXiv:hep-th/0605088 [hep-th].

[24] M. Fujita, K. Fukushima, T. Misumi, and M. Murata, Phys.Rev. **D80**, 035001 (2009), arXiv:0903.2316 [hep-ph]; M. Fujita, T. Kikuchi, K. Fukushima, T. Misumi, and M. Murata, Phys. Rev. **D81**, 065024 (2010), arXiv:0911.2298 [hep-ph].

[25] H. R. Grigoryan, P. M. Hohler, and M. A. Stephanov, Phys.Rev. **D82**, 026005 (2010), arXiv:1003.1138 [hep-ph].

[26] J. Erlich, E. Katz, D. T. Son, and M. A. Stephanov, Phys.Rev.Lett. **95**, 261602 (2005), arXiv:hep-ph/0501128 [hep-ph].

[27] A. Karch, E. Katz, D. T. Son, and M. A. Stephanov, Phys. Rev. **D74**, 015005 (2006), arXiv:hep-ph/0602229.

[28] D. Son and M. Stephanov, Phys.Rev. **D69**, 065020 (2004), arXiv:hep-ph/0304182 [hep-ph].

[29] P. M. Hohler, Phys.Rev. **D83**, 026005 (2011), arXiv:1010.2494 [hep-ph].

[30] C. P. Herzog, Phys. Rev. Lett. **98**, 091601 (2007), arXiv:hep-th/0608151.

[31] D. T. Son and A. O. Starinets, JHEP **0209**, 042 (2002), arXiv:hep-th/0205051 [hep-th]; C. P. Herzog and D. T. Son, *ibid.* **03**, 046 (2003), arXiv:hep-th/0212072.

[32] S. Caron-Huot, P. Kovtun, G. D. Moore, A. Starinets, and L. G. Yaffe, JHEP **0612**, 015 (2006), arXiv:hep-th/0607237 [hep-th].

[33] A. Nunez and A. O. Starinets, Phys. Rev. **D67**, 124013 (2003), arXiv:hep-th/0302026; P. K. Kovtun and A. O. Starinets, Phys.Rev. **D72**, 086009 (2005), arXiv:hep-th/0506184 [hep-th].

[34] X. Zhao and R. Rapp, Phys.Lett. **B664**, 253 (2008), arXiv:0712.2407 [hep-ph].

[35] H. Liu, K. Rajagopal, and U. A. Wiedemann, JHEP **0703**, 066 (2007), arXiv:hep-ph/0612168 [hep-ph].

[36] M. Stephanov and Y. Yin, JHEP **1202**, 017 (2012), arXiv:1111.5303 [hep-ph].

[37] G. Festuccia and H. Liu, (2008), arXiv:0811.1033 [gr-qc].

[38] J. Casalderrey-Solana and D. Mateos, Phys.Rev.Lett. **102**, 192302 (2009), arXiv:0806.4172 [hep-ph].

[39] R. C. Myers and A. Sinha, JHEP **0806**, 052 (2008), arXiv:0804.2168 [hep-th].

[40] A. Adare et al. (PHENIX Collaboration), Phys.Rev.Lett. **104**, 132301 (2010), arXiv:0804.4168 [nucl-ex].

[41] X. Zhao and R. Rapp, Phys.Rev. **C82**, 064905 (2010), arXiv:1008.5328 [hep-ph].